

Material Characterization of FRP Pre-Cured Laminates Used in the Mechanically Fastened FRP Strengthening of RC Structures

by A. Rizzo, N. Galati, A. Nanni, and L.R. Dharani

Synopsis: The Mechanically Fastened-FRP (MF-FRP) strengthening system consists of pre-cured FRP laminates having high longitudinal bearing strength attached to the concrete surface using closely spaced steel fasteners in the form of nails or concrete wedge anchors. The connection depends on several parameters such as, the intrinsic laminates properties (tensile and bearing strength), diameter and effective embedment length of the fasteners, clamping force, presence and type of washer, presence and type of filler in the gaps between the FRP material, the fastener and accessories, and the concrete. This paper focuses on the material characterization of pultruded pre-cured laminate which was used as MF-FRP strengthening to retrofit and rehabilitate off-system bridges in Missouri, USA. Tensile tests, in the longitudinal and transverse direction of the laminate, were performed on full section and open hole coupons in order to characterize the material. Bearing tests, in the longitudinal and transverse direction of the laminate, were performed to determine the capacity of the unrestrained fastener-FRP-concrete connection.

Keywords: flexural strengthening; material characterization; mechanically fastened FRP pre-cured laminates

136 Rizzo et al.

Andrea Rizzo is a PhD Candidate in Civil Engineering at the University of Lecce-Italy where he also received his B.Sc. in Materials Engineering. He obtained his M.Sc. degree in Engineering Mechanics at the University of Missouri-Rolla. His research interests include analysis and design of RC structures.

Nestore Galati is a research engineer at the University of Missouri-Rolla. He obtained his PhD in Civil Engineering at the University of Lecce-Italy where he also received his B.Sc. in Materials Engineering. He obtained his M.Sc. degree in Engineering Mechanics at the University of Missouri-Rolla. His research has concentrated on the area of retrofitting of masonry and upgrade and in-situ load testing of RC structures.

Antonio Nanni (FACI) is the V & M Jones Professor of Civil Engineering at the University of Missouri-Rolla. He is the founding Chair of ACI Committee 440, Fiber-Reinforced Polymer Reinforcement, and is the current Chair of ACI Committee 437, Strength Evaluation of Existing Concrete Structures. He is an active member in technical committees of ASCE (Fellow), ASTM, and TMS.

Lokeswarappa R. Dharani is professor of Engineering Mechanics and Aerospace Engineering, and Senior Investigator in Graduate Center for Materials Research, at the University of Missouri-Rolla. His research interests are micromechanics, composite materials, fatigue analysis, fracture mechanics, process modeling, wear and friction in composites, analysis and design of laminated glass units.

RESEARCH SIGNIFICANCE

The mechanical characterization of pultruded pre-cured laminate to be used in a Mechanically Fastened-FRP (MF-FRP) strengthening system is discussed. The critical parameters affecting design are investigated from a fundamental point of view, allowing for the development of FRP products usable for these types of applications.

INTRODUCTION

The Mechanically Fastened-FRP (MF-FRP) strengthening system has recently emerged as a practical alternative for the flexural strengthening of RC structures. The efficiency of this strengthening technique was demonstrated in terms of structural performances, and costs, labor and time savings by means of several laboratory (Borowicz 2002; Lamanna 2002; Arora 2003; Ekenel et al. 2005) and field applications. The first reinforced concrete bridge strengthening with the method was performed on a bridge in Edgerton, Wisconsin in 2002 (Bank et al. 2003). This was followed by applications on four rural bridges in Phelps and Pulaski Counties in Missouri (off-system project) in 2004 (Bank et al. 2004; Rizzo 2005).

Different issues were to be solved in the development of the FRP laminate to be mechanically fastened to RC members. The common existing pultruded strips intended to be adhesively bonded on the concrete surface are highly orthotropic in nature, possessing a high modulus and strength in the longitudinal direction, along the length of the

laminate, and a low modulus and strength in the transverse direction, across the width of the laminate. The lack of reinforcing fibers in the transverse direction causes these strips to splinter apart when a fastener is driven through them. The pre-cured FRP laminate trademarked under the name SafStrip™, used in the off-system project (Bank et al. 2004; Rizzo 2005), was designed, produced and commercialized as the result of an investigation performed by Lamanna (2002) having as objective the development of a high bearing strength FRP plate. It consists of a glass and carbon hybrid pultruded strip embedded in a vinyl ester resin. Its thickness and width are 3.175 mm and 101.6 mm, respectively. Continuous glass fiber strand mats are used to provide transverse and bearing strength, while 16-113 yield E-glass roving and 40-48K Grafil standard modulus carbon tows are utilized to provide longitudinal strength.

Table 1 summarizes the properties of the constituent materials (Arora 2003). Tensile tests were performed on 25.4 mm wide full section and open hole (having 4.775 mm diameter hole in the middle) coupons: the average stress at failure and the modulus of elasticity resulted 844.0 MPa and 61.3 GPa (Borowicz 2002; Lamanna 2002; Arora 2003), respectively. Unrestrained bearing tests were made using 4.775 mm and 12.7 mm diameter pins (the free edge distance was equal to 50.8 mm): the maximum load at failure was 3.99 kN and 9.45 kN, respectively, after the material around the bolt contact area crushed resulting in an elongation of the hole (bearing failure).

A powder-actuated fastening tool was adopted by the University of Wisconsin – Madison (UW) research team for all the laboratory and field applications, in order to increase the speed of installation of the FRP laminates (Borowicz 2002; Lamanna 2002; Arora 2003). The powder-actuated system consists of pins embedded into the base material by means of a gunpowder charge. The type of fasteners was chosen depending on the compressive strength of the concrete. Concrete spalling and cratering were reduced by pre-drilling 12.7 mm deep holes in the concrete. A neoprene backed washer was used to prevent localized crushing and provide a clamping pressure, which is known to significantly increase bearing strength in the vicinity of the hole (Camanho et al. 1997; Cooper et al. 1995; Wu et al. 1998). Anchor bolts having a 12.7 mm diameter replaced pins in vicinity of the supports to accommodate for the strip delamination at the ends and to obtain extended ductility of the structural elements (Arora 2003). Shear test of single connection showed a bearing mode of failure at a maximum load of 6.08 kN.

The use of the powder-actuated fastening system was found efficient for low compressive strength concrete in lab (Borowicz 2002; Lamanna 2002) and field (Arora 2003) application. Nevertheless, during the installation of the FRP strengthening on the field it was found that occasionally, fasteners did not fully penetrate the concrete substrate due to the presence of obstructions (such as large aggregates), and pocket of poor consolidation and/or deteriorated concrete (factors that can be easily controlled in a lab environment) caused loosening of nails. On the other hand, in cases of compressive concrete strength higher than 17.2 MPa, the fastening method resulted in concrete spalling and cratering which were considered not acceptable for the full engagement of the laminate. Therefore, the fastening method developed by Bank and Lamanna was modified for the Missouri off-system bridges characterized by high compressive concrete

strength and/or with large hard aggregates.

Renouncing the speed of powder-actuated system in order to have a system slower but more reliable, two different types of high strength anchor were tested: concrete wedge anchors and bolts of different size (see Fig. 1). Concrete wedge anchors are inserted into a hole drilled into concrete. The concrete wedge bolts are one piece, heavy duty anchors. The installation of wedge bolts is much easier and faster than the installation of wedge anchors since it only consists in driving it into predrilled holes.

Since the pre-cured FRP laminate SafStrip™ is a relatively new material, a consistent database of its properties was not available at the onset of the project. The values of tensile and bearing properties in literature were found just for 25.4 mm wide coupons, while the cross section of the laminate presents inhomogeneities that could affect the overall capacity of the strip. In addition, the documented open hole tensile strength was not completely defined since it referred to a fixed ratio between the width and the hole size of the coupon. Regarding the bearing capacity, the data available were related to the size of the particular fastener used and, therefore, they could not be adopted for different anchor diameters. Thus, it was needed to investigate the behavior of the laminate under the influence of the new connection geometric parameters chosen.

CHARACTERIZATION OF THE FRP PRE-CURED LAMINATE

Material characterization tests were conducted to determine key characteristics to the design of the strengthening system: tensile and bearing tests in the longitudinal and transverse directions, and open hole tensile tests in the longitudinal direction. For each type of test, different coupon geometries were analyzed and, if possible, at least three units for each type were tested. From pilot tests, it was observed that no tabs were necessary in order to prevent gripping damage.

Coupons were cut using common band and table saws. The bolt holes were machined using the special hole generation procedure developed at the Royal Institute of Technology in Stockholm (Persson 1997). The hole is generated with a cutting tool rotating eccentrically about a principal axis and, at the same time, about its own axis. Using this method, it is possible to machine holes with high precision without causing delamination and chip-out. Fig. 2 shows the conditions of the material around the holes corresponding to different procedures used to generate them. Delamination at the side of the holes, when a common rotary hammer drill bit was used, underlines the major problem associated with the drilling of fiber-reinforced composite materials. In addition to the reduction of the structural integrity of the material, drilling also results in poor assembly tolerance and potential deterioration of long-term performance.

Longitudinal tensile tests

Tensile tests according to ASTM D 3039 were conducted on the laminates to determine longitudinal elastic modulus and tensile strength. Since the cross section of the laminate is not homogeneous, specimens having width in the range 6.6 ÷ 77.3 mm were tested in order to analyze size effects on the mechanical behavior of the laminate. Both

ends of each sample were enclosed in the machine grips for a 76.2 mm length. An Instron 25.4 mm extensometer was clamped to the middle of each specimen.

Fig. 3 shows the representative failure modes observed in longitudinal tensile tests. The failure was explosive (see Fig. 3a) and occurred always in the gage length close to the middle of the specimens. The rupture started with single carbon fiber failures randomly distributed across the coupon width with subsequent delamination of the two external mat layers. The delamination was complete right before reaching the ultimate load. For coupons wider than 50.8 mm, some strips of carbon tows remained unbroken (see Fig. 3b): the number and the width of this strips increased with the width of the specimens.

The behavior of the material was linear elastic up to failure. The modulus of elasticity E was calculated according to ASTM D 3039 as the tensile cord modulus of elasticity within the strain range 1000 ÷ 3000 $\mu\epsilon$. The strain at failure ϵ_u was defined as the ratio between the stress at failure σ_u and the modulus E . It is possible to distinguish three different groups of coupons in which the stress at failure σ_u was about constant (see Table 2). The first and the second groups have about the same stress at failure but the former has a higher standard deviation. The third group consists of the wider coupons and it is characterized by the lowest value of stress at failure and relative standard deviation. The following observations can be made based on the tests results:

- the ultimate stress σ_u decreases by increasing of the width w ;
- the scattering of the ultimate stress σ_u decreases for higher values of the coupon widths w ;
- the modulus of elasticity E slightly decreases with the increasing of the width w ;
- there is no correlation between the strain at failure ϵ_u and the width w of the coupons;
- the results obtained in the longitudinal tensile tests are consistent with the theoretical ones calculated according to the mixture rule. The theoretical stress and strain at failure, and the elastic modulus are 1094 MPa, 17648 $\mu\epsilon$ and 62 GPa, respectively. The difference between the experimental and the theoretical results can be attributed to the presence of defects and premature failure modes that the theory does not take into account.

Transverse tensile tests

Transverse tensile tests according to ASTM D 3039 were conducted on the laminates to determine their elastic modulus and tensile strength in the transverse direction. Specimens having width in the range 14.1 ÷ 49.0 mm were used in order to analyze the size effects on the mechanical behavior of the laminate. Both ends of each sample were enclosed in the machine grips for a 12.7 mm length. An Instron 25.4 mm extensometer was clamped to the middle of some specimens.

Fig. 4 shows the representative type of failure for the transverse tensile tests. The failure was brittle and net across the entire width of the samples: it occurred always in the gage length of the specimens (see Fig. 4a). The rupture started with the appearance of one

140 Rizzo et al.

or more splitting cracks through the carbon fibers core along the load direction, cracks that propagate until the ultimate load was reached (see Fig. 4b): to be noted that, by visual inspection, no splitting cracks were detected running through the glass roving, showing that the glass fibers-vinyl ester mechanical interface is more efficient than the carbon fibers-vinyl ester one.

Fig. 5 depicts the average stress-strain ($\sigma - \varepsilon$) curve up to failure. It is possible to state that the behavior of the material in the transverse direction can be modeled as a parabola with satisfactory approximation. The following observations can be made based on the tests results (see Table 3):

- no correlation was found between the ultimate stress σ_u and the coupons width w ;
- the modulus of elasticity at origin E_o , calculated as the modulus at origin of the parabola that best fit the experimental stress-strain curve, increases with the increasing of the width w ;
- no correlation was found between the strain at failure ε_u and the width w of the coupons;
- the high scattering in the stress and strain at failure can be attributed to the particular lay-up of the laminate. The non regularity in the cross section could have caused stress concentration points from where cracks initiated and then propagated along the load direction (see Fig. 4b).

Longitudinal open hole tensile tests

Longitudinal open hole tensile tests according to ASTM D 5766 were conducted on the laminates to determine the properties in the longitudinal direction based on the coupons net section. Different specimens were tested to analyze the size effects on the mechanical behavior of the laminate. In particular, the ratio $\rho = w/\phi$, defined as the ratio between the width of the specimens w and the diameter of the holes ϕ , was varied in the range 1.27 to 12.0. Both ends of each sample were enclosed in the machine grips for a length equal to 63.5 mm. An Instron 25.4 mm extensometer was clamped to the middle of the samples.

Fig. 6 shows the representative type of failure for open hole longitudinal tensile tests (see

Table 4). The failure was brittle and explosive across the entire width of the samples: it occurred always in the gage length of the specimens with extensive splitting and delamination. The failure was always anticipated by single carbon fiber failures randomly distributed in the coupon width. Fig. 6a shows the pattern of the cracks around the hole in the outer layers for different coupons. In general, it was observed that:

- for ratios $w/\phi \cong 1.0 \div 1.5$, not appreciable cracking could be seen up to failure but, reached the ultimate load, the outer layers failed across the drilled section;
- for ratios $w/\phi \cong 2.0 \div 4.0$, a crack formed at the center of each quadrant of the hole and propagated at 45° reaching, in some cases, the side of the coupon deviating from the original toward the horizontal direction;

- for ratios $w/\phi > 4.0$, the cracks, formed at low load level, tended to propagate in the longitudinal direction marking the splitting of the carbon core starting from the hole edges (see also Fig. 6a);
- a visual inspection of the specimens after failure showed the splitting of a carbon strip wide as the hole size and running across all the half length of samples (see Fig. 6b). Fig. 7 and Fig. 8 plot the average stress at failure on the net area $\sigma_{u,n}$ as a function of the width of the coupons w and of the ratio w/ϕ , respectively.

Bearing tests in the longitudinal direction of the laminate

Double-shear tensile loading tests according to ASTM D 5961 Procedure A were conducted on the laminates to determine the bearing response in the longitudinal direction. For this group of tests, designated as series A, no clamping pressure was applied on the contact area pin-FRP material (unconstrained specimens). Specimens having ratios $w/\phi \in 2.7 \div 10.5$ and $e/\phi \in 0.8 \div 7.7$ were used to analyze the effect of the geometry on the mechanical behavior of the laminate. w and ϕ are the width of the coupon, and the hole size, respectively. e is the distance, parallel to load, from center of the hole to end of specimen. Fig. 9 shows the test setup used for the bearing tests. The particular fixtures allowed using pins of different size maintaining a clear sight of the hole deformation during the loading of the specimens. Because of the particular test setup and test machine available, it was possible to record just the data related to the load and the cross-head displacement.

Fig. 10 shows the representative type of failure for the series A longitudinal bearing tests. Mainly, two different modes of failure occurred depending on the ratios w/ϕ and e/w . Maintaining constant w/ϕ , for low values of e/w coupons failed along shear-out planes parallel to the load direction (see Fig. 10a), while for high values of e/w coupons failed for bearing in the material immediately adjacent to the contact area of pin and laminate (see Fig. 10b). The shear-out failure started with the appearance of two longitudinal cracks on the hole edges at both sides of the coupon; then, the cracks ran quickly up to the free edge of the specimen. No relevant damage was found at the outer layers in contact with the pin, while the inner carbon fibers layer split along the middle plane of the laminate (see Fig. 10c). Such mode of failure was less extensive for specimens having higher distance between hole and edge. The failure due to bearing has been shown to occur through buckling and brushlike failure with consequent delamination of the outer layers in the material far away from the contact area (see Fig. 10b): commonly, carbon fibers were push out in the final part of the test (see Fig. 10d).

According to ASTM D 953 and ASTM D 5961, the experimental results can be summarized in terms of maximum bearing stress $\sigma_{br,max}$, cross-head displacement at failure Δ_u for each group of specimens, bearing strength $\sigma_{br,u}$ and the bearing chord stiffness E_{br} . To be noted that generally, the bearing failure starts at the contact points in the 0° – direction and then propagates through the rest of the contact area. This means

142 Rizzo et al.

that the stress distribution on the contact area is not constant and that the effective maximum bearing stress is higher than the average value suggested by ASTM D 953 and calculated using the conventional bearing area. The hole opening δ was estimated subtracting the elastic deformation of the test apparatus from the cross-head displacement (Rizzo 2005). The following observations can be made based on the tests results (see Fig. 11 and Fig. 12 related to $\phi = 9.525 \text{ mm}$ and reported as example):

- the maximum bearing stress $\sigma_{br,max}$ strongly depends on the distance from the edge e . It is mildly influenced by the hole size ϕ , and it almost does not depend on the width w ;
- the maximum bearing stress $\sigma_{br,max}$ does not depend on the width of the coupons;
- by maintaining a constant diameter ϕ , there is a minimum value of the edge distance e_{min} beyond which the maximum bearing stress $\sigma_{br,max}$ assumes a constant value independently from the edge distance e and below which there is a linear correlation between $\sigma_{br,max}$ and e . Fixing an edge distance $e \leq e_{min}$, the maximum bearing stress $\sigma_{br,max}$ is slightly higher for smaller diameter size;
- no correlation was found between the edge distance e_{min} and the width of the coupons;
- the bearing chord modulus E_{br} is not affected by the width of the specimen and it tends to increase with the edge distance.

Double bearing tests in the longitudinal direction of the laminate

Double-shear tensile loading tests according to ASTM D 5961 Procedure A were conducted on the laminates to investigate the bearing response in the longitudinal direction in the presence of two holes at the same distance from the free edge. For this group of tests, designated as series B, no clamping pressure was applied on the contact area pin-FRP material (unconstrained specimens). The investigation was limited to specimens with full width of the laminate, and using 9.525 mm diameter holes spaced at 50.8 mm symmetrically with respect to the center of each specimen. Different values of edge distance were tested in order to analyze the effect of this geometrical parameter on the mechanical behavior of the laminate.

The mode of failure was bearing and occurred through buckling and brushlike failure with consequent delamination of the outer layers. The failure was not contemporaneous for both holes. The following observations can be made based on the tests results:

- the bearing chord modulus E_{br} tends to increase with the edge distance since more material reacts to the pressure of each pin;
- the maximum bearing stress $\sigma_{br,max}$ is independent from the edge distance e : $\sigma_{br,max} = 213.5 \pm 15.6 \text{ MPa}$. This value is slightly smaller (about 9%) than the maximum bearing stress found for the series A specimens;
- the curves $(\sigma_{br} - \varepsilon_{br})$ are generally linear up to $60 \div 80\%$ of the maximum bearing stress with a subsequent deviation to the linearity depending on the failure mode (the non

linearity is higher for bearing failure).

Bearing tests in the transverse direction of the laminate

Double-shear tensile loading tests according to ASTM D 5961 Procedure A were conducted on laminates to investigate the bearing response in the transverse direction. For this group of tests, designated as series C, no clamping pressure was applied on the contact area pin-FRP material (unconstrained specimens). Specimens having ratios $w/\phi \in 2.5 \div 10.0$ and $e/\phi \in 1.3 \div 3.8$ were tested to analyze the effect of the geometry on the mechanical behavior of the laminate.

Fig. 13 shows the representative type of failure for series C transverse bearing tests. The ratio e/w has no effect on the type of failure since the presence of the longitudinal carbon fiber prevents the premature shear-out failure. Therefore, mainly two different modes of failure occurred depending on the ratio w/ϕ . For low values of w/ϕ , coupons failed for net tension (see Fig. 13a): for the smaller width w , traces of bearing failure damages were localized in the material immediately adjacent to the contact area of pin and laminate. For high values of w/ϕ , coupons failed for bearing in the material immediately adjacent to the contact area of pin and laminate (see Fig. 13b): for the smaller width w , net tension failure occurred right after the bearing failure. The net tension failure started with the appearance of two transverse cracks on the hole boundary at both sides of the coupon; then, the cracks ran quickly up to the free edges of the specimen. By visual inspection, no relevant damages were found in the outer layers of material in contact with the pin, except for the specimens with the highest value of w for which the initial stage of the bearing failure process could developed due to the higher net tension capacity of the coupons. The failure due to bearing has been shown to occur through brushlike failure with consequent delamination of the outer layers. It is important to note that the damaged zone is less extensive than what found in the series A longitudinal bearing tests. In fact, in the transverse bearing tests, there is not buckling but the carbon fibers are just pushed in a more stable configuration creating a natural ring in the contact area against the pin, a fact that increased the post-bearing capacity until the final secondary net tension failure. The following observations can be made based on the tests results:

- the maximum bearing stress $\sigma_{br,max}$ depends on the geometry of the coupon: it strongly depends from the coupon width w (see Fig. 14), slightly from the edge distance e and mildly from the hole size ϕ ;
- the maximum bearing stress $\sigma_{br,max}$ depends on the width of the coupons (Fig. 14b);
- with a fixed diameter ϕ , there is a minimum value of the edge distance e_{min} beyond which the maximum bearing stress $\sigma_{br,max}$ assumes a constant value independently from the edge distance e and below which there is a linear correlation between $\sigma_{br,max}$ and e ;
- the edge distance e_{min} slightly depends on the hole size ϕ and tends to increase with the diameter;

144 Rizzo et al.

- the curves ($\sigma_{br} - \varepsilon_{br}$) are generally linear up to 75 ÷ 90% of the maximum bearing stress, while subsequent deviation to the linearity become more evident depending on the failure mode;
- the bearing capacity depends just on the contact area that the pin can provide. In fact, it was proved that the maximum bearing stress is constant for specimens of a certain hole size tested with pins of different size (Rizzo 2005).

CONCLUSIONS

Conclusions based on the material characterization tests of the SafStripTM pre-cured FRP laminate can be summarized as follows:

- the SafStripTM laminate behavior is linear elastic up to failure for tensile load in the longitudinal direction. For design purposes, the stress at failure and the elastic modulus found for full size specimens can be conservatively assumed to be 836 MPa and 62 GPa, respectively. The resultant strain at failure was found to be 13809 $\mu\varepsilon$;
- the SafStripTM laminate behavior can be modeled as a parabola for tensile load in the transverse direction: $\sigma_{av} [MPa] = -1.884 \cdot 10^{-7} \mu\varepsilon^2 + 7.151 \cdot 10^{-3} \mu\varepsilon$ with modulus at origin equal to $E_o = 7151 MPa$. In addition, no size effects on the mechanical behavior of the laminate for tensile load in the transverse direction have been observed. For design purpose, the average stress and the strain at failure can be conservatively assumed to be 65.6 MPa and 13498 $\mu\varepsilon$, respectively;
- the full size SafStripTM laminate containing a hole in the middle of the width behaves as the same laminate without hole. Therefore, for design purposes, the stress on the net area, the elastic modulus and the strain at failure for full size specimens with hole in the middle of the width can be assumed to be equal to the corresponding values found for full size specimens without hole, that is 836 MPa, 62 GPa and 13809 $\mu\varepsilon$, respectively. In addition, it is reasonable to state that the same conclusions are valid for full size (101.6 mm wide) laminates with a hole in a generic position along the width provided the ratio $w/\phi \geq 3$;
- the maximum bearing stress in the longitudinal direction for unconstrained material around the hole is equal to $235.2 \pm 17.2 MPa$ and it does not depend on the size of the hole. This value of bearing stress can be only reached by choosing an adequate value of the edge distance: according with the experimental results, the minimum edge distance that satisfied the previous requirement is about 25 mm;
- the maximum bearing stress in the transverse direction for unconstrained material around the hole is equal to $160.1 \pm 23.2 MPa$ and it can be considered independent from the size of the hole. This value of bearing stress can be reached only choosing an adequate value of the edge distance (15 mm for the tested laminate).

ACKNOWLEDGMENTS

The project was made possible with the financial support received from the UMR - University Transportation Center on Advanced Materials, Center for Infrastructure Engineering Studies at the University of Missouri-Rolla and Meramec Regional Planning Commission (MRPC). Strongwell provided the FRP materials.

REFERENCES

Arora, D., 2003, *Rapid Strengthening of Reinforced Concrete Bridge with Mechanically Fastened Fiber-Reinforced Polymer Strips*, Master's thesis, University of Wisconsin – Madison, WI.

ASTM D 953-02, 2002, *Standard Test Method for Bearing Strength of Plastics*, American Society for Testing and Materials, West Conshohocken, PA.

ASTM D 3039/D 3039M, 2000, *Standard Test Method for Tensile Properties of Polymer Matrix Composite Materials*, American Society for Testing and Materials, West Conshohocken, PA.

ASTM D 5766/D 5766M, 2002, *Standard Test Method for Open Hole Tensile Strength of Polymer Matrix Composite Laminates*, American Society for Testing and Materials, West Conshohocken, PA.

ASTM D 5961/D 5961M, 2001, *Standard Test Method for Bearing Response of Polymer Matrix Composite Laminates*, American Society for Testing and Materials, West Conshohocken, PA.

Bank, L.C.; Arora, D.; Borowicz, D.T.; and Oliva, M., 2003, "Rapid Strengthening of Reinforced Concrete Bridges," *Wisconsin Highway Research Program*, Report Number 03-06, 166 pp.

Bank, L.; Nanni, A.; Rizzo, A.; Arora, D.; and Borowicz, D., 2004, "Concrete Bridges Gain Strength with Mechanically Fastened, Pultruded FRP Strips," *Composites Fabrication Magazine*, September, pp. 32-40.

Borowicz, D. T., 2002, *Rapid Strengthening of Concrete Beams with Powder-Actuated Fastening Systems and Fiber-Reinforced Polymer (FRP) Composite Materials*, Master's thesis, University of Wisconsin – Madison, WI.

Camanho, P. P. and Matthews, F. L., 1997, "Stress Analysis and Strength Prediction of Mechanically Fastened Joints in FRP: a Review," *Composites Part A*, Vol. 28A, pp. 529-547.

Cooper, C. and Turvey, G. J., 1995, "Effects of Joint Geometry and Bolt Torque on the Structural Performance of Single Bolt Tension Joints in Pultruded GRP Sheet Material,"

146 Rizzo et al.

Composite Structures, Elsevier, Vol. 32, pp. 217-226.

Ekenel, M.; Rizzo, A.; Myers, J. J.; and Nanni, A., 2005, "Effect of Fatigue Loading on Flexural Performance of Reinforced Concrete Beams Strengthened with FRP Fabric and Pre-Cured Laminate Systems," *Conference of Composites in Construction*, Lyon, France.

Lamanna, A.J., 2002, *Flexural Strengthening of Reinforced Concrete Beams with Mechanically Fastened Fiber Reinforced Polymer Strips*, PhD thesis, University of Wisconsin – Madison, WI.

Persson, E.; Eriksson, I.; and Zackrisson, L., 1997, "Effects of Hole Machining Defects on Strength Fatigue Life of Composite Laminates," *Composites Part A*, 28A, pp. 141-151.

Rizzo, A., 2005, *Application in Off-System Bridges of Mechanically Fastened FRP (MF-FRP) Pre-Cured Laminates*, Master's thesis, University of Missouri-Rolla, MO.

Wu, T. J. and Hahn, H. T., 1998, "The Bearing Strength of E-Glass/Vinyl-Ester Composites Fabricated by VARTM," *Composites Science and Technology*, Vol. 58, pp. 1519-1529.

Table 1 -- Components Properties of the Pre-cured FRP Strip (Arora 2003)

Component	Tensile Elastic Modulus* [GPa]	Cross Sectional Area or Thickness* [mm ² / mm]	Tensile Ultimate Strength* [MPa]
16-113 Yield E-glass Roving	72.4	1.730 mm ²	3448
40-48K Standard Modulus Carbon Tows	234.5	1.778 mm ²	4137
42.5 gr Continuous Strand Mat	6.90	0.737 mm**	345
Vinyl Ester Resin	3.38	NA	81.4

*Obtained from manufacturers data.

**Mat thickness based on 552 kPa .

Table 2 -- Experimental Longitudinal Properties of the SafStripTM Laminate

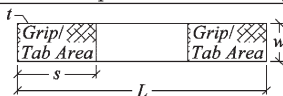
Coupons	Failure Stress σ_u [MPa]	Modulus of Elasticity E [GPa]	Strain at Failure $\epsilon_u = \frac{\sigma_u}{E}$ [$\mu\epsilon$]
6.6 mm ≤ w < 35 mm	950 ± 120	68.0 ± 32.4	14101 ± 1639
35 mm ≤ w < 60 mm	1002 ± 66	62.5 ± 4.2	16261 ± 1920
60 mm ≤ w ≤ 77.3 mm	836 ± 30	62.7 ± 7.6	13809 ± 1599
6.6 mm ≤ w ≤ 77.3 mm (Average Value)	937 ± 109	65.6 ± 5.9	14705 ± 1938
<i>Specimen without Hole for Longitudinal Tensile Test</i>			
		Grip Length $s = 76.2$ mm Thickness $t = 3.175$ mm Total Length $L = 381 \pm 5$ mm Width $w \in 6.6 \div 77.3$ mm	

Table 3 -- Experimental Transverse Properties of the SafStripTM Laminate

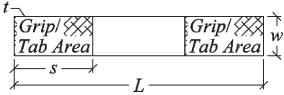
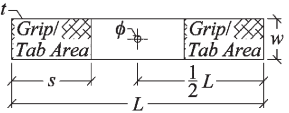
Coupons	Failure Stress σ_u [MPa]	Elastic Modulus at Origin E_o [GPa]	Strain at Failure ϵ_u [$\mu\epsilon$]
14.1 mm ≤ w < 49.0 mm	65.6 ± 14.5	6.765 ± 1.017	13498 ± 3940
<p><i>Specimen without Hole for Transverse Tensile Test</i></p>  <p>Grip Length $s = 12.7$ mm Thickness $t = 3.175$ mm Total Length $L = 101.6 \pm 0.5$ mm Width $w \in 14.1 \div 49.0$ mm</p>			

Table 4 -- Experimental Longitudinal Open Hole Properties of the SafStripTM Laminate

Coupons	Average Failure Stress At Failure $\sigma_{u,n} = \frac{P}{(w-\phi)t}$ [MPa]	Elastic Modulus E_{oh} [GPa]	Strain at Failure ϵ_u [$\mu\epsilon$]
$w/\phi = 6$; $w \leq 67.2$ mm	$-12.681 w [mm] + 991$	NA	NA
$w/\phi = 6$; $w > 67.2$ mm	787 ± 17	70.8 ± 3.0	11755 ± 1467
$\phi = 6.35$ mm; $w \geq 25.4$ mm	870 ± 91	66.4 ± 2.8	13503 ± 1090
$\phi = 9.525$ mm; $w \geq 25.4$ mm	882 ± 62	71.5 ± 3.3	12613 ± 226
Average Values for $w/\phi \geq 3$	898 ± 114	70.2 ± 3.9	12594 ± 1137
<p><i>Specimen with Hole for Longitudinal Open Hole Tensile Test</i></p>  <p>Grip Length $s = 63.5$ mm Thickness $t = 3.175$ mm Total Length $L = 381 \pm 5.8$ mm Width $w \in 12.2 \div 101.6$ mm Diameter $\phi \in 1.43 \div 12.81$ mm</p>			



a) Concrete Wedge Anchor



b) Concrete Wedge Bolt

Fig. 1 — Concrete Anchors

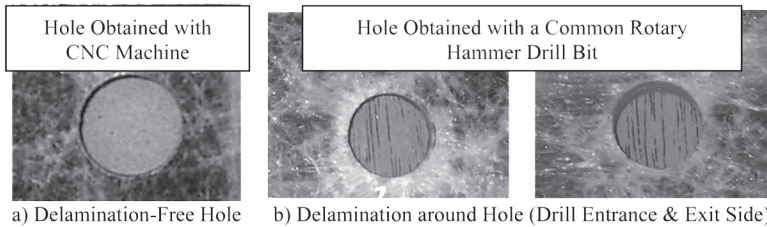
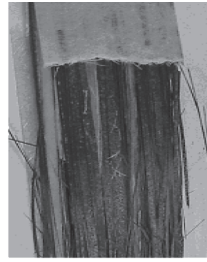


Fig. 2 — FRP Material Conditions around Holes

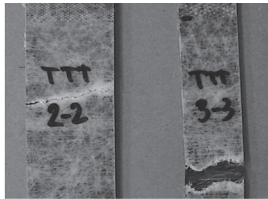


a) Explosive Failure

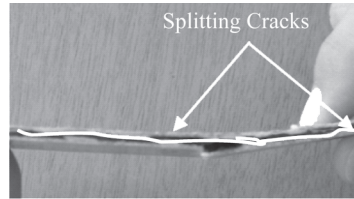


b) Failure Details for Coupons Wider than 50.8 mm

Fig. 3 — Failure Modes in Longitudinal Tensile Tests of SafStrip™ Coupons



a) Net Failure across the Width



b) Splitting Cracks through Carbon Fibers Core

Fig. 4 — Type of Failure for Transverse Tensile Tests of SafStrip™ Coupons

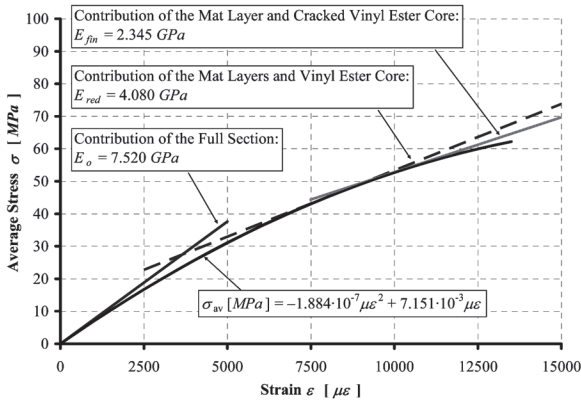


Fig. 5 — Average Stress-Strain ($\sigma - \epsilon$) Curve for Transverse Tensile Tests

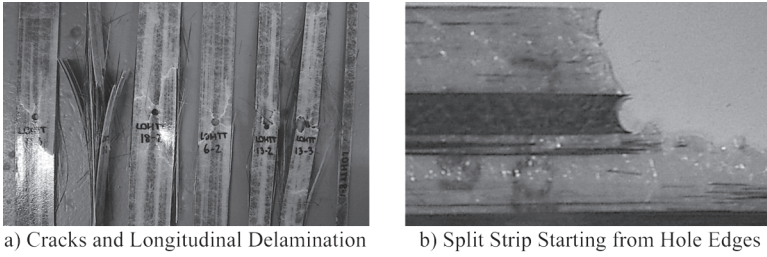


Fig. 6 — Type of Failure for Longitudinal Open Hole Tensile Tests of SafStrip™ Coupons

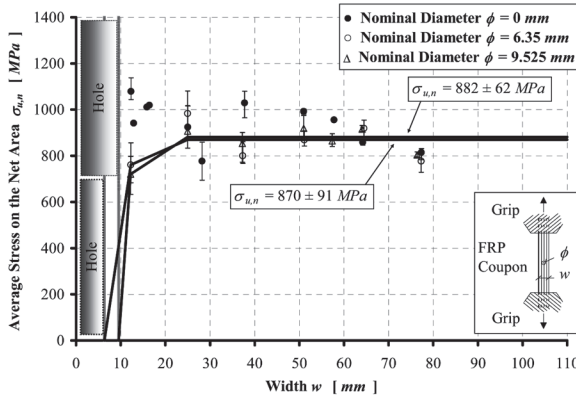


Fig. 7 — Stress at Failure on the Net Area $\sigma_{u,n}$ vs. Coupon Width w for Constant Hole Size for Longitudinal Open Hole Tensile Tests

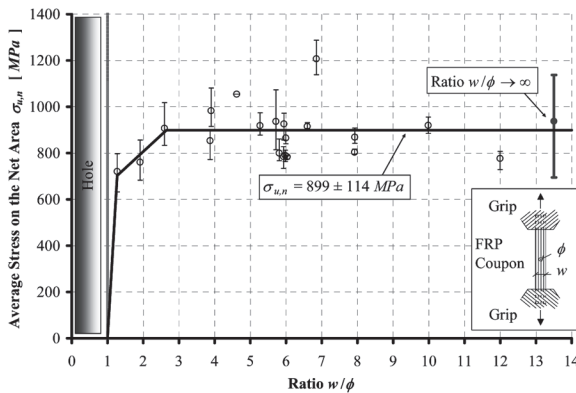


Fig. 8 — Stress at Failure on the Net Area $\sigma_{u,n}$ vs. Ratio w/ϕ for Longitudinal Open Hole Tensile Tests

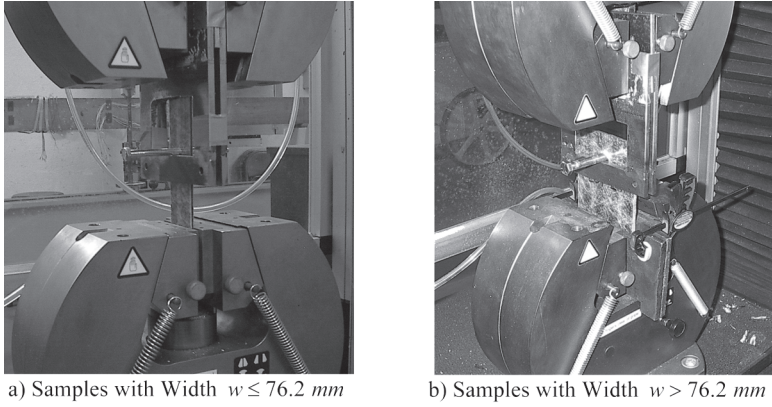


Fig. 9 — Bearing Tests Setup

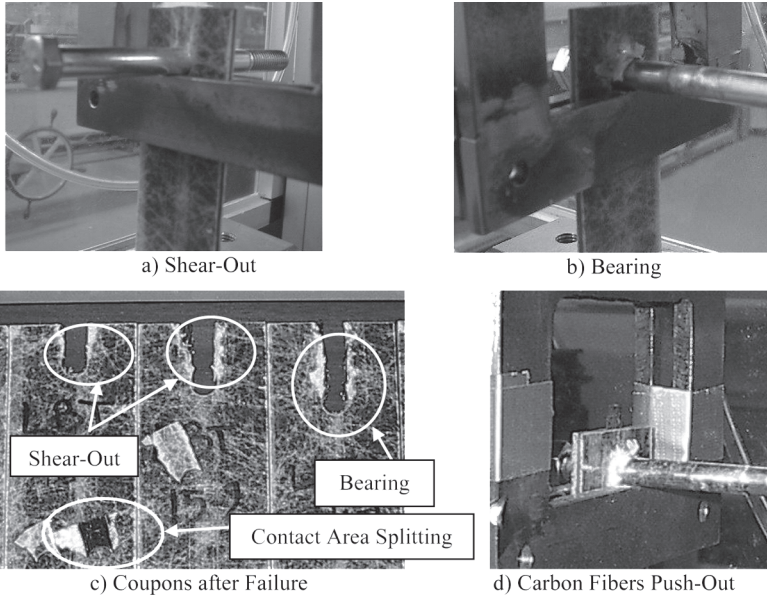


Fig. 10 — Type of Failure for Series A Longitudinal Bearing Tests of SafStrip™ Coupons

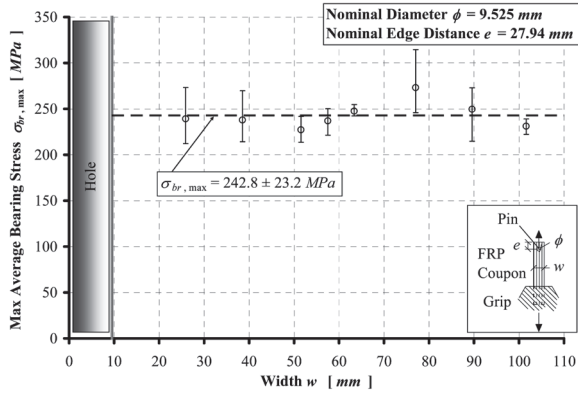
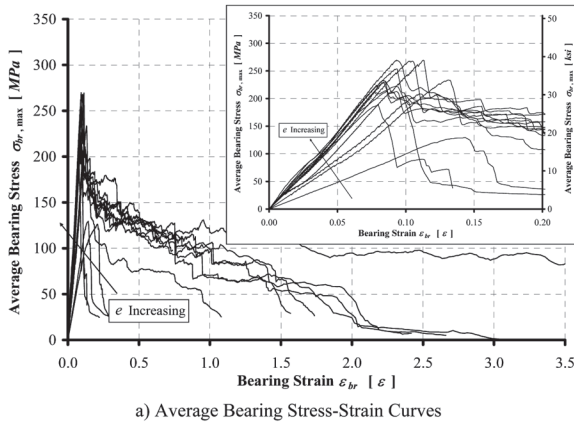
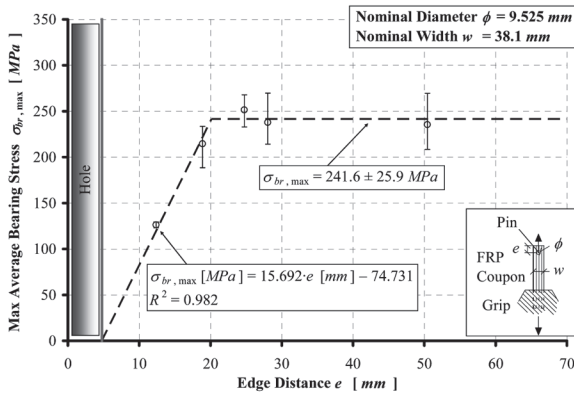


Fig. 11 – Series A Longitudinal Bearing Tests Results for w Variable, $\phi = 9.525\text{ mm}$ and $e = 27.94\text{ mm}$

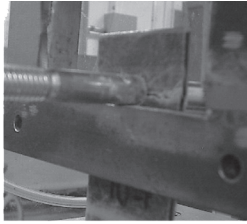


a) Average Bearing Stress-Strain Curves

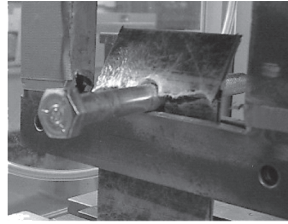


b) Maximum Average Bearing Stress

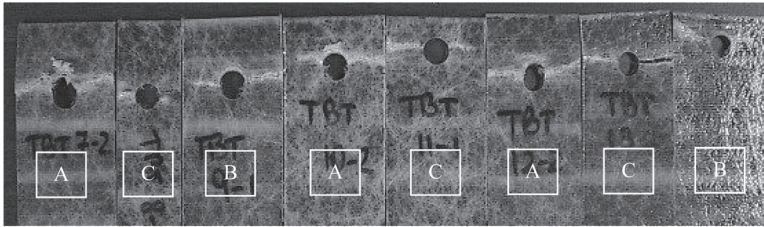
Fig. 12 – Series A Longitudinal Bearing Tests Results for e Variable, $\phi = 9.525\text{ mm}$ and $w = 38.1\text{ mm}$



a) Net Tension Failure without Bearing Traces



b) Net Tension Failure after Bearing



c) Coupons after Failure: Net Tension Failure with Severe (A), Minor (B) and Negligible (C) Bearing Damages in the Contact Area

Fig. 13 — Type of Failure for Series C Transverse Bearing Tests of SafStrip™ Coupons

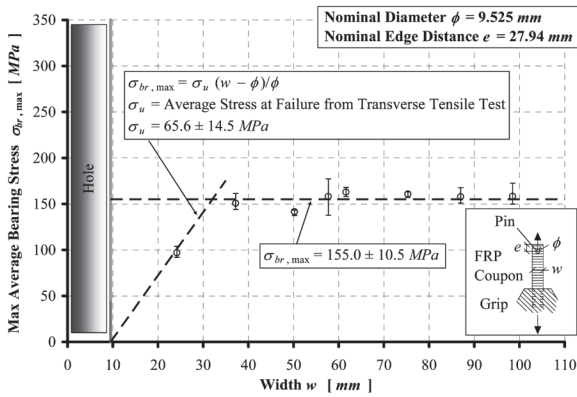


Fig. 14 — Series C Transverse Bearing Tests Results for w Variable, $\phi = 9.525 \text{ mm}$ and $e = 27.94 \text{ mm}$